Number of HIV-1 founder variants is determined by the recency of the source partner infection

Title: Number of HIV-1 founder variants is determined by the recency of the source partner infection

Authors: Ch. Julián Villabona-Arenas[1,2], Matthew Hall[3], Katrina A. Lythgoe[3], Stephen G. Gaffney[4], Roland R. Regoes[5], Stéphane Hué[1,2], Katherine E. Atkins[1,2,6 *]

Affiliations:

[1]Department of Infectious Disease Epidemiology, Faculty of Epidemiology and Population Health, London School of Hygiene and Tropical Medicine, London, UK
[2]Centre for Mathematical Modelling of Infectious Diseases, London School of Hygiene and Tropical Medicine, London, UK
[3]Big Data Institute, Nuffield Department of Medicine, University of Oxford, Oxford, UK
[4]Division of Biostatistics, Yale School of Public Health, New Haven, USA
[5]Institute of Integrative Biology, Department of Environmental Systems Science, ETH Zurich, Zurich, Switzerland
[6]Centre for Global Health, Usher Institute of Population Health Sciences and Informatics, The University of Edinburgh, Edinburgh, UK
* corresponding author: Katherine.Atkins@ed.ac.uk

One sentence summary: Multiple founder variant transmission of HIV-1 increased during early infection.

Abstract

During sexual transmission, the large genetic diversity of HIV-1 within an individual is frequently reduced to one founder variant that initiates infection. Understanding the drivers of this bottleneck is crucial to develop effective infection control strategies. Little is known about the importance of the source partner during this bottleneck. To test the hypothesis that the source partner affects the number of HIV founder variants, we developed a phylodynamic model calibrated using genetic and epidemiological data on all existing transmission pairs for whom the direction of transmission and the infection stage of the source partner are known. Our results suggest that acquiring infection from someone in the acute (early) stage of infection increases the risk of multiple founder variant transmission when compared with someone in the chronic (later) stage of infection. This study provides the first direct test of source partner characteristics to explain the low frequency of multiple founder strain infections.

Main Text

Sexual transmission of HIV-1 results in a viral diversity bottleneck due to physiological barriers as well as viral or cellular constraints that prevent most genetic variants within the source partner from establishing onward infection (*1–3*). Indeed, this diversity bottleneck results in around three quarters of new infections being founded by a single genetic variant (*4–9*). The extent of genetic diversity transmitted to a new partner is a crucial determinant in understanding the efficacy of putative vaccines and may shed light on the transmission of drug resistance to treatment naive individuals.

The factors leading to the diversity bottleneck during sexual transmission can be broadly categorized as those determined by the source partner—such as viral load and viral diversity available for transmission *(10)*, those determined by the recipient partner—such as target cell type and availability in the genital or rectal mucosa (e.g. (*3*, *11*, *12*)), and those connected with viral characteristics—such as glycosylation profiles and cell tropism (reviewed in (*13*)). While the impact of the recipient partner and the characteristics of transmitted founder variants have been widely discussed, little is known about how the source partner affects the viral diversity bottleneck. Modelling work suggests that infection stage of the source partner at the point of onward transmission may be a key driver in determining the number of transmitted variants (*14*). However, there is currently no empirical evidence to suggest how the infection stage of the source partner influences the viral diversity bottleneck. This gap has arisen because analyses are routinely conducted on individuals without information on the partner from whom they acquired infection. Phylogenetic analyses now offer a possible solution to this impasse.

Phylogenetic trees are representations of the ancestral relationships of organisms with the tips of the tree representing those that are sampled, the internal nodes representing their inferred common ancestors, and the branches as the evolutionary pathways between these actual and inferred individuals. When phylogenetic trees are constructed using sequence data from both partners in an HIV transmission pair, the relationship between the evolutionary histories of both sets of viral samples may reflect epidemiological relationships between the two individuals (*15-17*). Previous modelling studies suggest that the evolutionary histories of the viral populations in both partners can provide important information, such as the direction of transmission (*15*) and the number of transmitted founder variants (*18*). For this, each putative transmission pair can be classified into one of three 'topologies' that defines the evolutionary relationship between the viral populations of the two partners: monophyletic-monophyletic (*MM*, where the sequences from each partner form separate groups), paraphyletic-monophyletic (*PM*, where the sequences from one partner are embedded in the sequences from the second partner), or a combination of paraphyletic and polyphyletic (*PP*, where sequences from both partners are interspersed) (**Fig. 1A**). The number of monophyletic clusters in a PM (one) or PP (more than one) tree can be interpreted as the minimum number of transmitted founder variants. In practice, however, many factors may influence epidemiological interpretations from phylogenetic trees such as sampling times, sampling density of the viral populations and phylogenetic signal (*19, 20*).

Here we present a data-driven phylodynamic approach to overcome these empirical and methodological issues to evaluate the impact of the source partner's infection stage and route of exposure on the HIV diversity bottleneck (**Fig. 1B, C**). We first retrieved all available genetic and epidemiological information from published HIV sexual transmission pairs where the

direction of transmission is known, and kept for further analysis those pairs for whom transmission could be classified as having occurred in the source partner's acute stage (≤90 days after his/her infection) or chronic stage (later than 90 days after his/her infection). After further stratifying pairs into heterosexual (HET) and men-who-have-sex-with-men (MSM) risk groups, we found a significant difference in the timing of transmission between the two risk groups. Specifically, 10 of 36 MSM pairs were the result of acute stage transmission compared with 1 of 76 of HET pairs (**Fig. 2**).

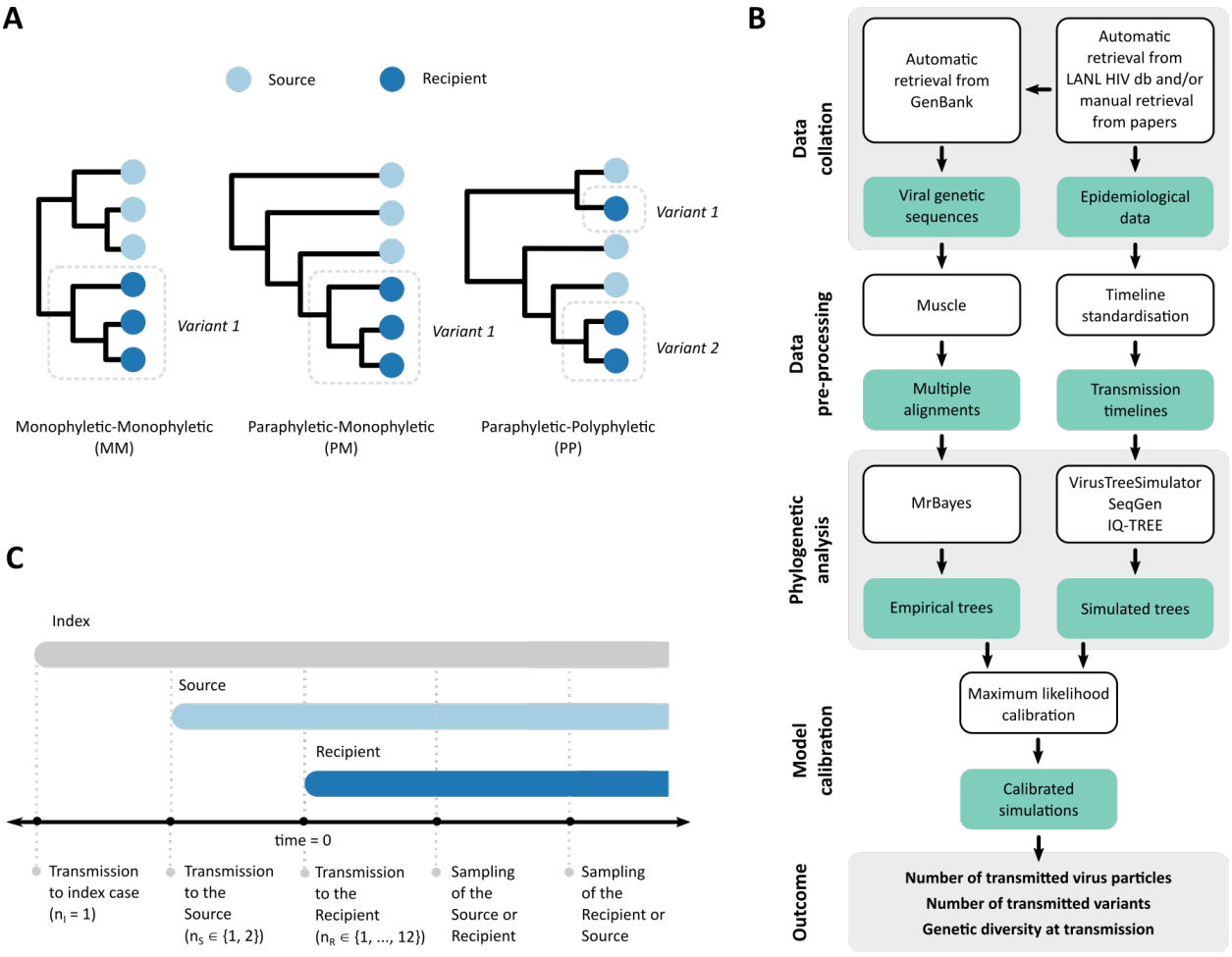

Fig. 1: Methods schematics. A) Phylogenetic tree topology class of known transmission pairs that have previously been used as a proxy for calculating the minimum number of founder variants transmitted to

the recipient: trees of class MM and PM both suggest a minimum of one founder variant while trees of class PP suggest a multiple founder variants, with the minimum number of founder variants being the number of recipient clades embedded in PP trees (here shown as two). B) Pipeline of phylodynamic analysis (LANLdb, Los Alamos National Laboratory HIV sequence database) where teal represents data or analysis output and white represents methods and analysis. An example of a standardised transmission timeline for a known source-recipient pair is provided in panel C. C) Schematic of the transmission pair model simulation that shows the transmission and sampling timelines. The simulated number of virus particles transmitted to the index case, and the source and recipient partners (n_I, n_S, n_R respectively) are shown on the transmission events timeline.

We then performed Bayesian phylogenetic tree reconstruction on the genetic sequences of the transmission pairs and classified the topology class of each tree in the posterior distribution as monophyletic-monophyletic (MM), paraphyletic-monophyletic (PM) or paraphyletic-polyphyletic (PP). The most likely topology class was PM (65% and 61% for HET and MSM, respectively), but with a higher number of PP trees in the MSM group (P=0.056, **Fig. 2**). This result has previously been reported as indicative of a higher number of founder variants for MSM (*18*). However, when we stratify the topology class by whether the source partner was in acute or chronic infection at the time of transmission, our results indicate that the infection stage of the source is the primary driver for any observed differences in topology class. Specifically, there is no difference between the HET and MSM groups in the PM/PP topology class ratio when transmission occurs in the chronic stage of infection (P=0.570). Note that only one HET transmission occurs during the acute stage, and the topology class for this pair is PP. These results remain qualitatively consistent when only data were analysed from the 66% of

transmission pairs for whom the posterior trees gave a certainty of over 95% for the most frequent topology class (**Fig. S3**). These results indicate that infection stage of the source partner, and not risk group *per se*, influences the diversity bottleneck at transmission.

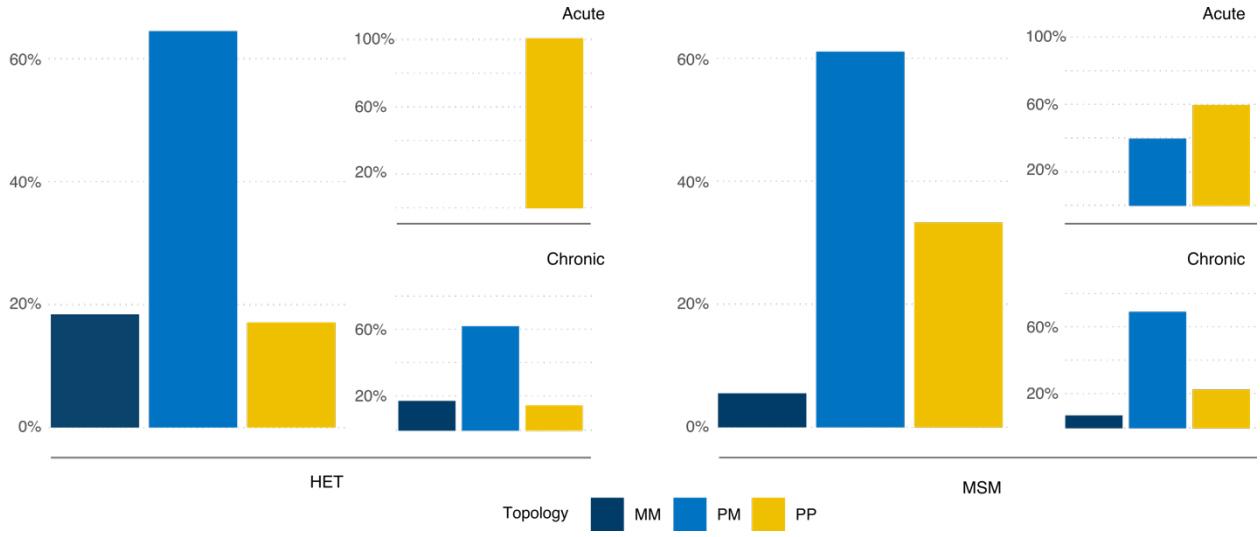

Fig. 2: Phylogenetic findings from the empirical transmission pairs. Fraction of phylogenetic tree topology class (MM: Monophyletic-Monophyletic, PM: Paraphyletic-Monophyletic and PP: Paraphyletic-Polyphyletic) where each tree topology class is classified as the most frequent topology class of each posterior distribution per transmission pair. Results are stratified by risk group: 76 heterosexual (HET) pairs and 36 men-who-have-sex-with-men (MSM) pairs) and infection stage of the source partner at transmission (11 acute pairs defined as <90d post infection and 101 chronic pairs defined as ≥90d post infection).

To test whether these empirical findings are indicative of a smaller diversity bottleneck in the chronic stage of HIV infection, we developed a phylodynamic framework in which we simulated the epidemiologic characteristics of each HET and MSM transmission pair, the timing of their sequence sampling, the transmission of virus particles, and the within-host genetic evolution in

both the source and recipient (**Fig. 1B)**. Specifically, using the epidemiological information from the transmission pairs, we simulated phylogenies under a coalescent model before generating genetic sequences from these simulations and performing Maximum Likelihood (ML) phylogenetic reconstruction on these simulated sequences. We classified each of these simulated trees as MM, PM or PP and determined the frequency of each topology class (*i.e.* the fraction of simulated trees that are classified as MM, PM and PP) for each simulated transmission pair across all the simulated sequences. However, as we could not directly observe the number of virus particles that are transmitted between source and recipient, we repeated the simulation of phylogenetic trees for each transmission pair under a range of plausible values of virus particles transmitted. By fitting the simulation output topology class distribution to the topology class distribution from the empirical phylogenetic trees using maximum likelihood inference, we then determined the most likely number of transmitted virus particles for each transmission pair and used this best fit model for further analysis. Note that two or more virus particles may have the same genetic sequence and would constitute a single founder variant (or haplotype), discussed later. Further, due to the analysis conditioning on extant lineages, we use the term 'founder variants' to describe those transmitted variants that found detectable viral lineages, thereby ignoring variants that are transmitted but the lineages of which become extinct.

Our fitting procedure selects a best fit model that clearly delineates between transmission pairs between whom one virus particle is transmitted (75% of pairs) and those between whom more than one virus particle is transmitted (25% of pairs, **Fig. 3A**). While there is a high degree of confidence in the result when one particle is transmitted, there is often uncertainty around the exact number when multiple particles are transmitted (**Fig. 3A**). Importantly, we found acute stage transmissions are more likely to lead to multiple particle infections compared with chronic

stage transmissions (73% vs. 20%, $P = 0.0005$). The topology class of the simulated phylogenetic trees is strongly influenced by the number of virus particles being transmitted (**Fig. 3B**). PM trees are more commonly found in the pairs that are better described by a model with a single transmitted virus particle (81%) whereas PP trees appeared more often when multiple particles are likely to have been transmitted (86%).

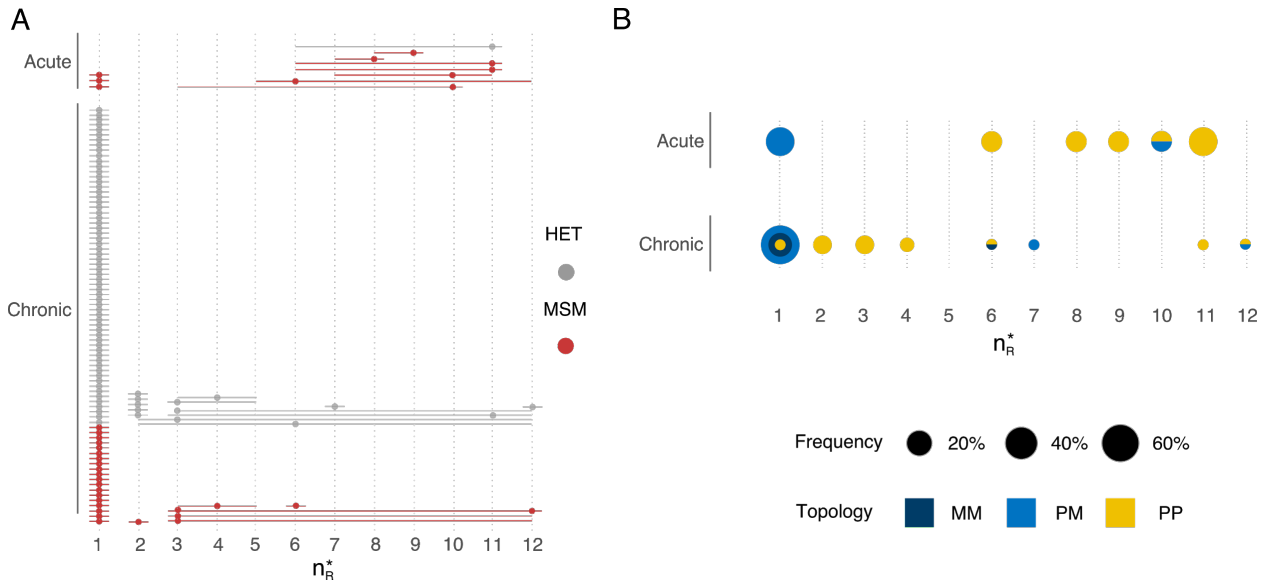

Fig. 3: **The estimated number of transmitted virus particles for the 112 transmission pairs.** The estimates of transmitted virus particles for each transmission pair were calculated by choosing the model simulation that generated a phylogenetic tree topology class distribution (that is, the number of MM, PM and PP trees constructed from the simulated genetic sequences) that best matched the topology class distribution from the phylogenetic trees constructed from the empirical genetic sequences. A) Maximum likelihood number of virus particles founding recipient infections, n_R^*, for each pair (stacked points) with 95% confidence intervals (lines) grouped by stage of infection (acute, 11 pairs or chronic, 101 pairs) and risk group (76 heterosexual pairs, HET and 36 men-who-have-sex-with-men pairs, MSM). B) Maximum

likelihood number of virus particles founding recipient infections coloured by topology class of the phylogenetic tree constructed from the simulated genetic sequences.

For each transmission pair, we then simulated the genetic sequences of the transmitted viral population under the best fit virus particle model and calculated the most likely number of founder variants for each transmission pair (*i.e.* the number of distinct haplotypes). The median number of founder variants transmitted across all pairs is 1 (range: 1-11, **Fig. 4A**). Using the full distribution of the number of transmitted founder variants for each pair, we also calculated the probability that a single founder variant was transmitted to the respective recipient. Our results suggest that across all pairs in both risk groups, the mean probability of observing one founder variant is 0.73. Stratifying by risk group, we find there is a higher probability that one founder variant founds HET infections than MSM infections (a geometric mean of 0.80 vs. 0.63, **Fig. 4B**). However, these risk group differences mostly disappear when we stratify the results by the infection stage of the source. Here, for example, when only chronic stage transmissions are considered, there is no difference in the probability of one founder variant between MSM transmissions and HET transmissions (means of 0.80 vs 0.71, P=0.398), and the pairwise diversity at transmission is similar between both groups (**Fig. 4C**). In contrast, when stratifying solely by infection stage of the source partner, we find that transmission during the acute stage has a much lower probability of one founder variant than during the chronic stage (means of 0.40 vs. 0.77) with a higher median number of founder variants transmitted, when only the most likely number of founder variants for each pair is considered (2 vs. 1, **Fig. 4A**). Nonetheless, if multiple founder variant transmission does occur, our results suggest that the number of founder variants

190 is higher during chronic stage transmission, consistent with a higher diversity measure during
191 this later stage of infection (**Fig. 4C**).

192 From these results, therefore, there is approximately double the chance of multiple founder
193 variant transmission during acute stage infection across both risk groups (relative risk = 0.52).
194 Assuming that transmission risk is weighted towards early transmission such that half of all
195 index case to source partner transmissions occur after 90 days of index case infection leads to
196 qualitatively similar results (Supplementary Materials). Similarly, calibrating the simulation
197 model to bootstrapped samples rather than Bayesian posterior distributions leads to similar
198 results (Supplementary Materials).
199
200 Our results suggest that there is an association between tree topology class and multiple founder
201 variant transmission, with 95% of MM and PM trees being due to one founder variant (**Fig. 4D**).
202 However, the number of embedded recipient clades is not always a proxy for the minimum
203 number of founder variants transmitted. For example, in chronic stage transmission, 11% of PP
204 topology class trees were due to single founder variant transmission (**Fig. 4D**). It is important to
205 stress that a PP topology class outcome may occur not only due to multiple genetically distinct
206 virus populations founding recipient infections but may also reflect a lack of phylogenetic signal
207 in the data; for instance, the sampled sequence lengths that gave rise to PP trees was on average
208 shorter than those for MM (P=0.096) and PM (P=0.004). Across both infection stages, we find
209 that if MM, PM or PP is assigned as the most likely tree topology class, then 92%, 96% and 15%
210 of transmissions are due to a single founder variant, respectively.
211

212 We have used a combination of empirical data and phylodynamic model simulation to evaluate
213 the role of infection stage at transmission and route of transmission on the number of virus
214 particles transmitted during sexual HIV exposure. This makes three important advances on
215 previous work. First, it is the first empirically-based study that fits a model to data to understand
216 the role of the source partner in multiple founder variant transmission. Second, while we use
217 previously developed topology classification of phylogenetic trees to understand HIV
218 transmission pairs, we extend this methodology by calibrating a phylodynamic model to
219 empirical data. This new approach provides a means to validate the untested assumption that the
220 number of embedded recipient partner lineages in a phylogenetic tree directly corresponds to the
221 minimum number of founder variants transmitted. Third, our phylodynamic model explicitly
222 incorporates virus particle number and the identity of genetic sequences. This advance produces
223 results that contrast with previous work that has shown the number of founder variants has little
224 impact on the topology class of the phylogenetic tree when only overall genetic diversity, rather
225 than sequence identity, is tracked (*15*).
226
227 The relative importance of acute and chronic stages of HIV in determining both the number of
228 virus particles and the number of founder variants transmitted is consistent with a recent
229 modelling study (*14*). However, our study finds higher proportions of infections initiated by
230 multiple founder variants overall during these two stages. This difference is likely due to the
231 assumptions related to how the stages of infection are defined as well as the relative importance
232 of transmission during late infection. Specifically, the previous modelling study finds that two
233 thirds of multiple founder variant transmission occurs during the pre-AIDS stage of infection
234 which is assumed to have both a high viral load and large haplotype diversity. If later stages of

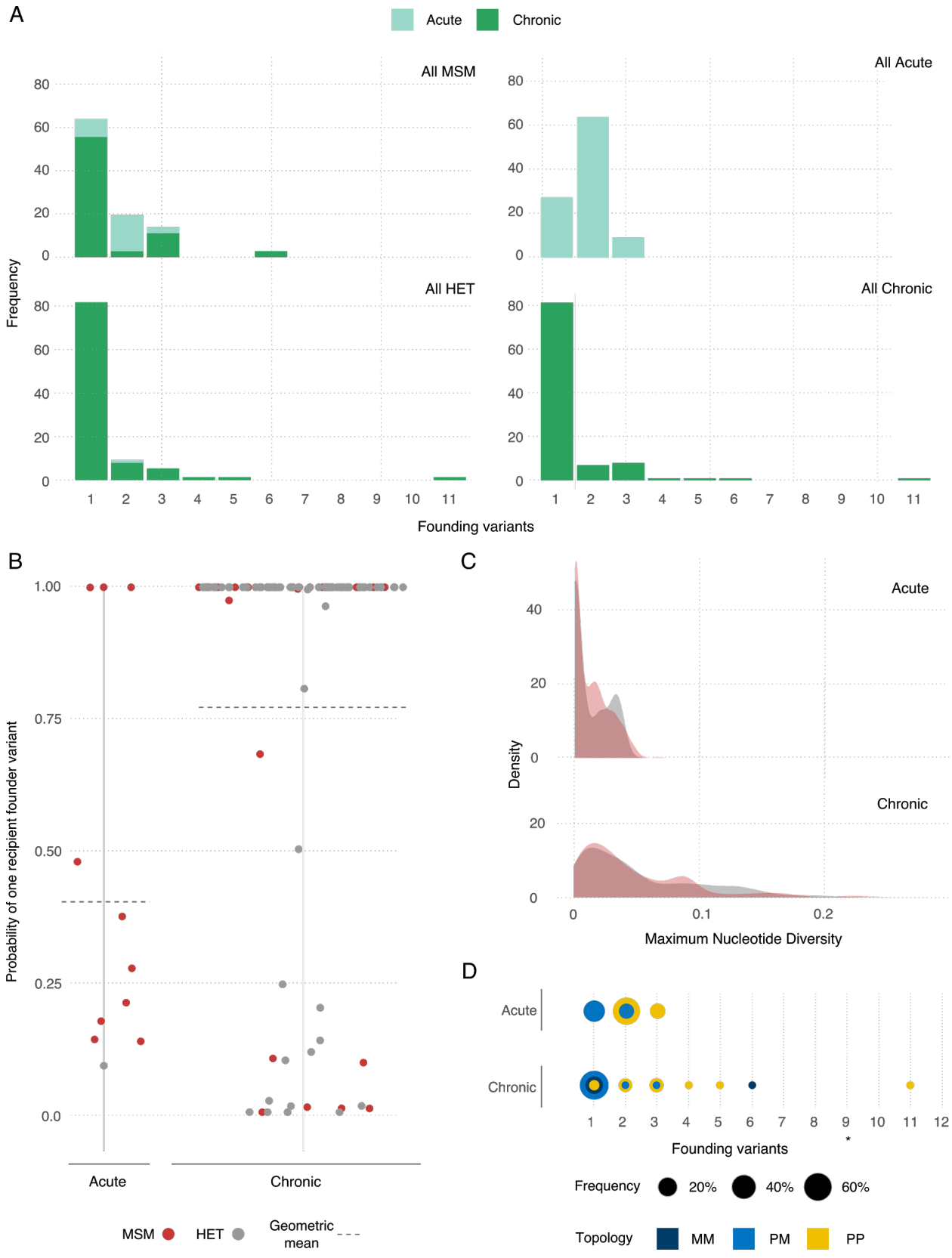
A
Acute
Chronic
All MSM
All Acute
All HET
All Chronic
Frequency
Founding variants
B
Probability of one recipient founder variant
Acute
Chronic
MSM
HET
Geometric mean
C
Acute
Chronic
Density
Maximum Nucleotide Diversity
D
Acute
Chronic
Founding variants
Frequency
20%
40%
60%
Topology
MM
PM
PP

235

Fig. 4: **Phylogenetic findings from the calibrated simulations**. A) Frequency of number of transmitted founder variants for transmission pairs by either infection stage of source partner at transmission (left) or risk group (right). The number of multiple founder variants is calculated as the modal simulated value. B) Probability of one founder variant in the recipient for each pair stratified by infection stage of the source partner at transmission. C) Probability density distribution of maximum diversity (proportion of sites that differ) in the recipient partner across all simulations with more than one haplotype stratified by infection stage of the source at transmission. D) Number of founder variants coloured by topology class of the phylogenetic tree constructed from the best fit model of the simulated genetic sequences.

infection account for disproportionately less transmission then the previous model would predict higher proportions of multiple founder variant transmission in both the acute and chronic stages of infection, becoming more consistent with empirical estimates from our analysis. By contrast, our study is agnostic about the relative importance of early and late transmission and does not differentiate between chronic and a pre-AIDS stage of infection, which cannot easily be identified through analysis of empirical data.

Data from four of the MSM transmission pairs in this study have previously been used to estimate the number of variants founding infection using a combination approach of single genome amplification (SGA), direct amplicon sequencing and mathematical modelling (*7*). Our results broadly agree with this previous analysis, with both analyses suggesting two recipients were infected with one founder variant and one recipient was infected with multiple founder variants (our analysis suggests a mean of 2-3 founder variants and the previous analysis suggests 3 founder variants); there was disagreement with results from a fourth recipient, for whom a

single founder variant was 13% probable in this study (with a mode of 2 founder variants) but the most likely outcome in the previous analysis. Small differences likely arise because this study uses sequence data from both partners to evaluate the transmission of multiple founder variants to the recipient partner. These extra data can be used to parameterize a mathematical model that accounts for the evolutionary relationship between the virus samples from both partners, rather than relying solely on accumulating diversity. Specifically, neglecting the extent of genetic similarity between the source and recipient virus samples might misattribute borderline cases of diversity accumulation.

Our study finds a median of one founder variant and a maximum of 11, with little difference between HET and MSM risk groups. When only multiple founder variant transmissions are considered, our study finds a median of 2-3 founder variants. These values are consistent with a previous pooled analysis using results from four analyses that used the current gold-standard SGA combination approach as above (*9*).

At present, the genetic determinants of HIV-1 disease progression are not clear. However, it is important to note that even small differences between genotypes can have important clinical outcomes. For instance, single polymorphisms can affect replication capacity (*21*), or can lead to primary non-nucleoside reverse transcriptase inhibitor resistance with different amino acids changes at the same position conferring equivalent levels of resistance (*22*).

Previous studies have disagreed over the extent to which the elevated risk of transmission during the acute stage of infection (reviewed in (*23*)) is driven by increased viral load, elevated per particle transmission probability or other behavioural factors such as high rates of sex partner change or concurrent partnerships (*24-29*). Here, while we find strong evidence to support the

fact that acute stage transmissions are characterised by more virus particles and variants founding infection, this result alone cannot disentangle virus- and host-related drivers of elevated transmission. For example, the higher number of variants being transmitted during acute infection could arise if the number of transmissible variants declines as infection progresses or, because with more particles being transmitted, there are more opportunities for multiple variants to found infection (*14,30*) However, our study can shed light on the eight times elevated per-exposure risk of infection that has been found for MSM relative to HET transmission (*31-32*). In particular, the lack of difference in both the number of virus particles and the number of founder variants that establish infection after transmission from a chronically infected source in HET and MSM suggests that the observed heightened acquisition risk for MSM could in part be due to sampled MSM individuals being more likely to be in the acute stage at the time of transmission (*14, 27*). Whether MSM partners are more likely to be sampled earlier in infection because of sampling procedures or because MSM are indeed more likely to transmit during early infection is unclear. While this observation raises the possibility that the role of sexual risk group in itself may have less of an impact on the transmission of multiple founder variant probability, from a pragmatic perspective, if more MSM infections are indeed caused by acute stage transmissions, the evolutionary and epidemiologic impact on public health will be the same irrespective of the mechanism.

There are two primary limitations to acknowledge. First, our model assumes a single transmission event between each source and recipient partner. Without detailed knowledge of the transmission pairs, we cannot distinguish between multiple infections each with a single founder variant and a single infection with multiple founder variants; if for some pairs, the former were

304 true then this might suggest an elevated transmission rate during the acute stage, as has been
305 observed previously (*28*, *29*). Second, our phylodynamic framework does not account for the
306 effect of selection and recombination. Specifically, selection, such as that for viruses which use
307 the CCR5 co-receptor (*33*), is thought to occur at the point of transmission , although the strength
308 may be dependent on the route of transmission (*34*).
309
310 Our study finds that the transmission of multiple HIV-1 founder variants is determined by
311 infection stage of the source partner, with transmission of more founder variants of HIV-1 in
312 acute compared with chronic infections. These findings stress that epidemiological or clinical
313 analysis of known transmission pairs should account for potential mediation by stage of
314 transmission when evaluating the effect of sexual risk group.
315
316 **Acknowledgements**

317 **Funding:** CJVA and KEA were funded by an ERC Starting Grant (award number 757688)
318 awarded to KEA. KAL was supported by The Wellcome Trust and The Royal Society grant no.
319 107652/Z/15/Z. MH was funded by The HIV Prevention Trials Network (grant number
320 H5R00701.CR00.01) and The Bill and Melinda Gates Foundation (grant number OPP1175094).
321 **Author contributions:** KEA conceived the study. CJVA, MH, KL, SH, KEA designed the
322 study. CJVA performed the experiments and analysed the data. CJVA, MH, KL, SH, KEA
323 interpreted the data. SGG created new software used in the study. KEA and CJVA drafted the
324 manuscript, with critical revisions from MH, RRR, KL, SH. All authors approved the final
325 version of the manuscript. **Competing interests:** The authors declare no competing interests.
326 **Data and materials availability:** All code and data are available at github.com/AtkinsGroup in

their respective repositories: data on the transmission pairs and sequence alignments (TransmissionPairs_Data), code for retrieval of transmission pair epidemiological data and metadata from Los Alamos National Laboratory HIV sequence database (TransmissionPairs_LANLRetrieval), code for sequence retrieval from GenBank (TransmissionPairs_GenBankRetrieval), code for phylodynamic analysis (TransmissionPairs_PhylodynamicAnalysis), and code for topological classification (TransmissionPairs_TreeTopologyAnalysis).

List of Supplementary Materials

Materials and Methods

Supplementary Text

Figs. S1 to S5

Data S1 to S4

References (*35-46*)

Reproducibility Checklist

References and Notes

1. J. L. Geoghegan, A. M. Senior, E. C. Holmes, Pathogen population bottlenecks and adaptive landscapes: overcoming the barriers to disease emergence. Proc. Biol. Sci. 283 (2016), doi:10.1098/rspb.2016.0727.
2. S. M. Kariuki, P. Selhorst, K. K. Ariën, J. R. Dorfman, The HIV-1 transmission bottleneck. Retrovirology. 14 (2017), , doi:10.1186/s12977-017-0343-8.
3. K. Talbert-Slagle, K. E. Atkins, K.-K. Yan, E. Khurana, M. Gerstein, E. H. Bradley, D. Berg, A. P. Galvani, J. P. Townsend, Cellular superspreaders: an epidemiological perspective on HIV infection inside the body. PLoS Pathog. 10, e1004092 (2014).
4. B. F. Keele, E. E. Giorgi, J. F. Salazar-Gonzalez, J. M. Decker, K. T. Pham, M. G. Salazar, C. Sun, T. Grayson, S. Wang, H. Li, X. Wei, C. Jiang, J. L. Kirchherr, F. Gao, J. A. Anderson, L.-H. Ping, R. Swanstrom, G. D. Tomaras, W. A. Blattner, P. A. Goepfert, J. M. Kilby, M. S. Saag, E. L. Delwart, M. P. Busch, M. S. Cohen, D. C. Montefiori, B. F. Haynes, B. Gaschen, G. S. Athreya, H. Y. Lee, N. Wood, C. Seoighe, A. S. Perelson, T. Bhattacharya, B. T. Korber, B. H. Hahn, G. M. Shaw,

Identification and characterization of transmitted and early founder virus envelopes in primary HIV-1 infection. Proc. Natl. Acad. Sci. U. S. A. 105, 7552–7557 (2008).

5. J. F. Salazar-Gonzalez, E. Bailes, K. T. Pham, M. G. Salazar, M. B. Guffey, B. F. Keele, C. A. Derdeyn, P. Farmer, E. Hunter, S. Allen, O. Manigart, J. Mulenga, J. A. Anderson, R. Swanstrom, B. F. Haynes, G. S. Athreya, B. T. M. Korber, P. M. Sharp, G. M. Shaw, B. H. Hahn, Deciphering human immunodeficiency virus type 1 transmission and early envelope diversification by single-genome amplification and sequencing. J. Virol. 82, 3952–3970 (2008).

6. M.-R. Abrahams, J. A. Anderson, E. E. Giorgi, C. Seoighe, K. Mlisana, L.-H. Ping, G. S. Athreya, F. K. Treurnicht, B. F. Keele, N. Wood, J. F. Salazar-Gonzalez, T. Bhattacharya, H. Chu, I. Hoffman, S. Galvin, C. Mapanje, P. Kazembe, R. Thebus, S. Fiscus, W. Hide, M. S. Cohen, S. A. Karim, B. F. Haynes, G. M. Shaw, B. H. Hahn, B. T. Korber, R. Swanstrom, C. Williamson, CAPRISA Acute Infection Study Team, Center for HIV-AIDS Vaccine Immunology Consortium, Quantitating the multiplicity of infection with human immunodeficiency virus type 1 subtype C reveals a non-poisson distribution of transmitted variants. J. Virol. 83, 3556–3567 (2009).

7. H. Li, K. J. Bar, S. Wang, J. M. Decker, Y. Chen, C. Sun, J. F. Salazar-Gonzalez, M. G. Salazar, G. H. Learn, C. J. Morgan, J. E. Schumacher, P. Hraber, E. E. Giorgi, T. Bhattacharya, B. T. Korber, A. S. Perelson, J. J. Eron, M. S. Cohen, C. B. Hicks, B. F. Haynes, M. Markowitz, B. F. Keele, B. H. Hahn, G. M. Shaw, High Multiplicity Infection by HIV-1 in Men Who Have Sex with Men. PLoS Pathog. 6, e1000890 (2010).

8. S. Gnanakaran, T. Bhattacharya, M. Daniels, B. F. Keele, P. T. Hraber, A. S. Lapedes, T. Shen, B. Gaschen, M. Krishnamoorthy, H. Li, J. M. Decker, J. F. Salazar-Gonzalez, S. Wang, C. Jiang, F. Gao, R. Swanstrom, J. A. Anderson, L.-H. Ping, M. S. Cohen, M. Markowitz, P. A. Goepfert, M. S. Saag, J. J. Eron, C. B. Hicks, W. A. Blattner, G. D. Tomaras, M. Asmal, N. L. Letvin, P. B. Gilbert, A. C. DeCamp, C. A. Magaret, W. R. Schief, Y.-E. A. Ban, M. Zhang, K. A. Soderberg, J. G. Sodroski, B. F. Haynes, G. M. Shaw, B. H. Hahn, B. Korber, Recurrent Signature Patterns in HIV-1 B Clade Envelope Glycoproteins Associated with either Early or Chronic Infections. PLoS Pathogens. 7 (2011), p. e1002209.

9. D. C. Tully, C. B. Ogilvie, R. E. Batorsky, D. J. Bean, K. A. Power, M. Ghebremichael, H. E. Bedard, A. D. Gladden, A. M. Seese, M. A. Amero, K. Lane, G. McGrath, S. B. Bazner, J. Tinsley, N. J. Lennon, M. R. Henn, Z. L. Brumme, P. J. Norris, E. S. Rosenberg, K. H. Mayer, H. Jessen, S. L. Kosakovsky Pond, B. D. Walker, M. Altfeld, J. M. Carlson, T. M. Allen, Differences in the Selection Bottleneck between Modes of Sexual Transmission Influence the Genetic Composition of the HIV-1 Founder Virus. PLoS Pathog. 12, e1005619 (2016).

10. K. A. Lythgoe, C. Fraser, New insights into the evolutionary rate of HIV-1 at the within-host and epidemiological levels. Proc. Biol. Sci. 279, 3367–3375 (2012).

11. B. F. Keele, J. D. Estes, Barriers to mucosal transmission of immunodeficiency viruses. Blood. 118 (2011), pp. 839–846.

12. L. R. McKinnon, R. Kaul, Quality and quantity. Current Opinion in HIV and AIDS. 7 (2012), pp. 195–202.

13. M. Sagar, Origin of the transmitted virus in HIV infection: infected cells versus cell-free virus. J. Infect. Dis. 210 Suppl 3, S667–73 (2014).
14. R. N. Thompson, C. Wymant, R. A. Spriggs, J. Raghwani, C. Fraser, K. A. Lythgoe, Link between the numbers of particles and variants founding new HIV-1 infections depends on the timing of transmission. Virus Evol. 5 (2019), doi:10.1093/ve/vey038.
15. E. O. Romero-Severson, I. Bulla, T. Leitner, Phylogenetically resolving epidemiologic linkage. Proc. Natl. Acad. Sci. U. S. A. 113, 2690–2695 (2016).
16. O. Ratmann, M. K. Grabowski, M. Hall, T. Golubchik, C. Wymant, L. Abeler-Dörner, D. Bonsall, A. Hoppe, A. L. Brown, T. de Oliveira, A. Gall, P. Kellam, D. Pillay, J. Kagaayi, G. Kigozi, T. C. Quinn, M. J. Wawer, O. Laeyendecker, D. Serwadda, R. H. Gray, C. Fraser, PANGEA Consortium and Rakai Health Sciences Program, Inferring HIV-1 transmission networks and sources of epidemic spread in Africa with deep-sequence phylogenetic analysis. Nat. Commun. 10, 1411 (2019).
17. C. Wymant, M. Hall, O. Ratmann, D. Bonsall, T. Golubchik, M. de Cesare, A. Gall, M. Cornelissen, C. Fraser, STOP-HCV Consortium, The Maela Pneumococcal Collaboration, and The BEEHIVE Collaboration, PHYLOSCANNER: Inferring Transmission from Within- and Between-Host Pathogen Genetic Diversity. Mol. Biol. Evol. 35, 719–733 (2018).
18. T. Leitner, E. Romero-Severson, Phylogenetic patterns recover known HIV epidemiological relationships and reveal common transmission of multiple variants. Nat Microbiol. 3, 983–988 (2018).
19. R. Rose, M. Hall, A. D. Redd, S. Lamers, A. E. Barbier, S. F. Porcella, S. E. Hudelson, E. Piwowar-Manning, M. McCauley, T. Gamble, E. A. Wilson, J. Kumwenda, M. C. Hosseinipour, J. G. Hakim, N. Kumarasamy, S. Chariyalertsak, J. H. Pilotto, B. Grinsztejn, L. A. Mills, J. Makhema, B. R. Santos, Y. Q. Chen, T. C. Quinn, C. Fraser, M. S. Cohen, S. H. Eshleman, O. Laeyendecker, Phylogenetic Methods Inconsistently Predict the Direction of HIV Transmission Among Heterosexual Pairs in the HPTN 052 Cohort. J. Infect. Dis. 220, 1406–1413 (2019).
20. A. B. Abecasis, M. Pingarilho, A.-M. Vandamme, Phylogenetic analysis as a forensic tool in HIV transmission investigations. AIDS. 32, 543-554. (2017).
21. D. B. A. Ojwach, D. MacMillan, T. Reddy, V. Novitsky, Z. L. Brumme, M. A. Brockman, T. Ndung'u, J. K. Mann, Pol-Driven Replicative Capacity Impacts Disease Progression in HIV-1 Subtype C Infection. J. Virol. 92 (2018), doi:10.1128/JVI.00811-18.
22. R. W. Shafer, J. M. Schapiro, HIV-1 drug resistance mutations: an updated framework for the second decade of HAART. AIDS Rev. 10, 67–84 (2008).
23. W. C. Miller, N. E. Rosenberg, S. E. Rutstein, K. A. Powers, Role of acute and early HIV infection in the sexual transmission of HIV. Curr. Opin. HIV AIDS. 5, 277–282 (2010).
24. E. M. Volz, E. Ionides, E. O. Romero-Severson, M.-G. Brandt, E. Mokotoff, J. S. Koopman, PLoS Med., 10(12): e1001568 (2013).
25. J. P. Hughes, J. M. Baeten, J. R. Lingappa, A. S. Magaret, A. Wald, G. de Bruyn, J. Kiarie, M. Inambao, W. Kilembe, C. Farquhar, C. Celum, Partners in Prevention HSV/HIV Transmission Study Team, Determinants of per-coital-act HIV-1 infectivity among African HIV-1-serodiscordant couples. J. Infect. Dis. 205, 358–365 (2012).

26. R. H. Gray, M. J. Wawer, R. Brookmeyer, N. K. Sewankambo, D. Serwadda, F. Wabwire-Mangen, T. Lutalo, X. Li, T. vanCott, T. C. Quinn, Rakai Project Team, Probability of HIV-1 transmission per coital act in monogamous, heterosexual, HIV-1-discordant couples in Rakai, Uganda. Lancet. 357, 1149–1153 (2001).
27. T. D. Hollingsworth, R. M. Anderson, C. Fraser, HIV-1 transmission, by stage of infection. J. Infect. Dis. 198, 687–693 (2008).
28. S. E. Bellan, J. Dushoff, A. P. Galvani, L. A. Meyers, Reassessment of HIV-1 acute phase infectivity: accounting for heterogeneity and study design with simulated cohorts. PLoS Med. 12, e1001801 (2015).
29. T. D. Hollingsworth, C. D. Pilcher, F. M. Hecht, S. G. Deeks, C. Fraser, High Transmissibility During Early HIV Infection Among Men Who Have Sex With Men-San Francisco, California. J. Infect. Dis. 211, 1757–1760 (2015).
30. K. A. Lythgoe, A. Gardner, O. G. Pybus, J. Grove, Short-Sighted Virus Evolution and a Germline Hypothesis for Chronic Viral Infections. Trends in Microbiology. 25 (2017), pp. 336–348.
31. M.-C. Boily, R. F. Baggaley, L. Wang, B. Masse, R. G. White, R. J. Hayes, M. Alary, Heterosexual risk of HIV-1 infection per sexual act: systematic review and meta-analysis of observational studies. Lancet Infect. Dis. 9, 118–129 (2009).
32. R. F. Baggaley, R. G. White, M.-C. Boily, HIV transmission risk through anal intercourse: systematic review, meta-analysis and implications for HIV prevention. Int. J. Epidemiol. 39, 1048–1063 (2010).
33. M. Beretta, A. Moreau, M. Bouvin-Pley, A. Essat, C. Goujard, M.-L. Chaix, S. Hue, L. Meyer, F. Barin, M. Braibant, ANRS 06 Primo Cohort, Phenotypic properties of envelope glycoproteins of transmitted HIV-1 variants from patients belonging to transmission chains. AIDS. 32, 1917–1926 (2018).
34. J. M. Carlson, M. Schaefer, D. C. Monaco, R. Batorsky, D. T. Claiborne, J. Prince, M. J. Deymier, Z. S. Ende, N. R. Klatt, C. E. DeZiel, T.-H. Lin, J. Peng, A. M. Seese, R. Shapiro, J. Frater, T. Ndung'u, J. Tang, P. Goepfert, J. Gilmour, M. A. Price, W. Kilembe, D. Heckerman, P. J. R. Goulder, T. M. Allen, S. Allen, E. Hunter, HIV transmission. Selection bias at the heterosexual HIV-1 transmission bottleneck. Science. 345, 1254031 (2014).
35. M. S. Cohen, C. L. Gay, M. P. Busch, F. M. Hecht, The Detection of Acute HIV Infection. The Journal of Infectious Diseases. 202 (2010), pp. S270–S277.
36. R. C. Edgar, MUSCLE: a multiple sequence alignment method with reduced time and space complexity. BMC Bioinformatics. 5, 113 (2004).
37. R. C. Edgar, MUSCLE: multiple sequence alignment with high accuracy and high throughput. Nucleic Acids Res. 32, 1792–1797 (2004).
38. F. Ronquist, J. P. Huelsenbeck, MrBayes 3: Bayesian phylogenetic inference under mixed models. Bioinformatics. 19, 1572–1574 (2003).
39. J. P. Huelsenbeck, F. Ronquist, MRBAYES: Bayesian inference of phylogenetic trees. Bioinformatics. 17, 754–755 (2001).
40. O. Ratmann, E. B. Hodcroft, M. Pickles, A. Cori, M. Hall, S. Lycett, C. Colijn, B. Dearlove, X. Didelot, S. Frost, A. S. M. M. Hossain, J. B. Joy, M. Kendall, D. Kühnert, G. E. Leventhal, R. Liang, G. Plazzotta, A. F. Y. Poon, D. A. Rasmussen, T. Stadler, E. Volz, C. Weis, A. J. Leigh Brown, C. Fraser, PANGEA-HIV Consortium,

Phylogenetic Tools for Generalized HIV-1 Epidemics: Findings from the PANGEA-HIV Methods Comparison. Mol. Biol. Evol. 34, 185–203 (2017).
41. A. Rambaut, N. C. Grassly, Seq-Gen: an application for the Monte Carlo simulation of DNA sequence evolution along phylogenetic trees. Comput. Appl. Biosci. 13, 235–238 (1997).
42. S. Alizon, C. Fraser, Within-host and between-host evolutionary rates across the HIV-1 genome. Retrovirology. 10, 49 (2013).
43. L.-T. Nguyen, H. A. Schmidt, A. von Haeseler, B. Q. Minh, IQ-TREE: a fast and effective stochastic algorithm for estimating maximum-likelihood phylogenies. Mol. Biol. Evol. 32, 268–274 (2015).
44. S. Kalyaanamoorthy, B. Q. Minh, T. K. F. Wong, A. von Haeseler, L. S. Jermiin, ModelFinder: fast model selection for accurate phylogenetic estimates. Nat. Methods. 14, 587–589 (2017).
45. S. R. Cole, H. Chu, S. Greenland, Maximum likelihood, profile likelihood, and penalized likelihood: a primer. Am. J. Epidemiol. 179, 252–260 (2014).
46. S. S. Iyer, F. Bibollet-Ruche, S. Sherrill-Mix, G. H. Learn, L. Plenderleith, A. G. Smith, H. J. Barbian, R. M. Russell, M. V. P. Gondim, C. Y. Bahari, C. M. Shaw, Y. Li, T. Decker, B. F. Haynes, G. M. Shaw, P. M. Sharp, P. Borrow, B. H. Hahn, Resistance to type 1 interferons is a major determinant of HIV-1 transmission fitness. Proc. Natl. Acad. Sci. U. S. A. 114, E590–E599 (2017).

Supplementary Materials for:

Number of HIV-1 founder variants is determined by the recency of the source partner infection

Ch. Julián Villabona-Arenas, Matthew Hall, Katrina A. Lythgoe, Stephen G. Gaffney, Roland R. Regoes, Stéphane Hué, Katherine E. Atkins

Correspondence to: Katherine.Atkins@ed.ac.uk

This PDF file includes:

Other Supplementary Materials for this manuscript include the following:

Data S1 to S4: SITable_EpiGeneticData.csv, SITable_AnalysisData.csv, SITable_ColumnNamesKey.csv, Alignments.zip, Reproducibility checklist

Materials and Methods

Data collation on linked transmission pairs

We automatically retrieved all HIV sequence data for men-who-have-sex-with-men (MSM) and heterosexual (HET) HIV transmission pairs for whom the direction of transmission is reported from The Los Alamos National Laboratory (LANL) HIV sequence database up to February

2019, such that each transmission pair comprise a 'source' and a 'recipient' partner. For each partner in the transmission pair we collected the following clinical and epidemiological data: (i) date of infection or time of infection prior to sampling, (ii) date of seroconversion or date of seroconversion prior to sampling, (iii) Fiebig stage at the time of sampling, (iv) date of sampling or time of sampling prior to infection, (v) number of sequences, (vi) genomic region, (vii) HIV subtype, and (viii) reported risk group. For each set of these transmission pair data we estimated, relative to the transmission time to the recipient partner (time = 0): (*i*) the time of transmission to the source partner, (*ii*) the time of the sampling of the source partner, and (*iii*) the time of sampling for the recipient partner (**Fig. 1**, Supplementary Text). We excluded all transmission pairs from further analysis for whom these three times could not be determined or for whom either partner has fewer than five sequences for all sampling times. For our base case analysis, we used the longest available genomic region with five or more sequences per partner. If more than one sampling time is available for any of the individuals, we selected the sample closest in time to the recipient infection.

Epidemiological data and sequence retrieval

For the ease of replicating our results and using existing transmission pair data for other purposes, we developed a Python script to automatically retrieve epidemiological and metadata for each transmission pair from the Los Alamos National Laboratory HIV sequence database (LANLdb). This script downloads the following data from both the source and recipient partners to a .csv file using as input the cluster and patients ids from LANLdb: (i) time of infection, (ii) time of seroconversion, (iii) Fiebig stage at the time of sampling, (iv) number of sequences, (v) genomic region, (vi) HIV subtype, (vii) reported risk group and (viii) GenBank accession IDs.

Next we used the downloaded GenBank accession IDs to automatically retrieve (ix) viral genetic sequences and (x) sampling dates (calendar dates) from GenBank using an R script. If information from (i) to (x) were missing for any individual, we manually retrieved these values from the original manuscripts where possible.

Completed datatables from these automatic and manual processes are provided at github.com/AtkinsGroup.

Transmission timelines

For each transmission pair, we define time = 0 as the time of recipient infection. We then calculated, using the data table retrieved, i) the time of infection of the source, ii) the time of sampling of the source, iii) the time of sampling of the recipient.

To estimate these times, we first calculated days from infection for both the source and the recipient partners. When these values are not given explicitly, we calculated them from time since seroconversion estimates or from Fiebig staging results. Specifically, we interpret seroconversion as the individual reaching Fiebig stage III (ELISA positive) that occurs between 22-37 days after infection and Fiebig stages I (viral RNA positive) and II (18-34) occurring 13 days and 28 days after infection, respectively (*35*). For all the pairs where a range of possible values is calculated, and for when a calendar month is provided, we incorporated the uncertainty around the infection and sampling times by assuming all values in these ranges are equally plausible and uniformly sampled within these range to account for the uncertainty.

For some pairs, the source was classified as ‘recent’ or ‘late’ at the time of transmission to the recipient partner. In these cases, we do not have an exact point to call time = 0. Therefore, for these pairs, for each simulation, we sample with replacement the time between source and recipient infections from the other pairs for whom we have previously classified as acute (<90 days delay), and chronic (90 days or more delay), sampling from the same risk group (MSM or HET) in each case.

All calculations, corresponding notes and final transmission times for each pair are provided at github.com/AtkinsGroup and visualised in **Fig. S1**.

Fig. S1: Infection and sampling times of the source and recipient for all the 112 transmission pairs analysed. Individual points denote exact times and lines denote uniform uncertainty in times. Source

partners points/lines overlapping the green shaded area correspond to transmission pairs for whom transmission occurs during the acute stage.

Empirical transmission pair analysis

Tree reconstruction: For each of the included transmission pairs, we generated posterior sets of phylogenetic trees. For this, we first constructed alignments using Muscle v3.8.31 (*36, 37*) with subtype specific reference sequences retrieved from the LANL HIV sequence database. Using these alignments, we built phylogenetic trees with MrBayes 3.2.7 (*38, 39*) under the assumption of a general time-reversible (GTR) nucleotide substitution model with the addition of invariant sites (I) and a gamma distribution of site rates. We constrained sequence data to be monophyletic with respect to the reference sequences to root the tree but ingroup relationships were unconstrained to avoid any topology class bias. We ran two Markov chains each with 30 million iterations, from which we sampled every 3,000th after discarding the first 50% as burn-in which provided an average standard deviation of split tree frequencies of below 0.01 or an effective sample size of greater than 300. This gave an empirical posterior distribution of $N = 5{,}000$ sample trees. In a sensitivity analysis, we tested the alternative method of using maximum likelihood phylogenetic tree reconstruction with bootstrapping.

Empirical topology class: We classified each of the resulting phylogenetic trees in the posterior distribution as either monophyletic-monophyletic (MM), or paraphyletic-monophyletic (PM), or paraphyletic-polyphyletic (PP), to reflect the cladistic relationship between the lineages from both individuals (Supplementary Text). Each transmission pair,k, is then described as a triplet of probabilities, D_k, denoting the frequency of each topology class within the kth pair's posterior

distribution $D_k = \{d_k(t)\}_{t \in T} = \{\Pr(t \mid k)\}_{t \in T}$ where $\sum_{t \in T} \Pr(t|k) = 1$ and $T \in \{\text{MM}, \text{PM}, \text{PP}\}$.

Simulated transmission pair analysis

We simulated the transmission of virus particles and within-host evolution, accounting for the epidemiological characteristics for each transmission pair. For each transmission pair, we simulated a chain of three HIV infections: (*i*) an unsampled index case who infected the source after three years of their own infection during their chronic stage to reflect that the majority of both HET and MSM transmission pairs transmitted during the chronic stage (101/112 pairs). In a sensitivity analysis we accounted for the assumption that transmission rate may be higher during the acute stage, with half of the index to source transmissions occurring after 90 days and the remaining half after three years, (*ii*) the source individual of the transmission pair, and (*iii*) finally the recipient individual of the transmission pair. For each individual within each trio, we simulated viral phylogenies that reflect between- and within-host viral evolution using VirusTreeSimulator (*40*), using as input the respective epidemiological and clinical information (Supplementary Text). We used a within-host effective population size consistent with that parameterized by the PANGEA-HIV study with the following logistic model parameters: initial effective population size (N_0) is 1, viral generation time (τ) is 1.8 days, effective population per year growth rate (r) is 2.85022, and time to half the carrying capacity of the viral population (t_{50}) is 2 years (*40*). For each transmission pair, we simulated a dated viral phylogeny that has the same number of tips as the number of retrieved sequences per partner and that is sampled at the respective sampling times for the source and recipient partner (Supplementary Text). For each recipient partner infection, we assume that a total of n_R virus particles founded the

129 infection. For each simulation, we further assume a total of n_S virus particles founding infection
130 of the source. We assume n_R takes values between one and a maximum of 12 and varied n_S
131 between one and two (Supplementary Text). We assume that the virus samples from each
132 recipient is representative of the within-host diversity, and that each founding virus particle has
133 an extant lineage. Therefore, we first assigned each sample (tip) of a phylogeny as a descendant
134 of one of the $n_R$virus particles. If there were more than 12 samples then the remaining tips were
135 assigned randomly to the $n_R = 12$ virus particles. If there were fewer than 12 samples, then we
136 constrained the number of founding virus particles, n_R, to equal the number of samples. For
137 every transmission pair, and for each value of n_R and n_S, we simulated 100 viral phylogenies.
138
139 For every simulated viral phylogeny, we simulated transmitted sequences by adding dummy
140 nodes with a negligibly short branch length after the transmission time. We then simulated the
141 evolution of nucleotide sequences along the tree using Seq-Gen (*41*) and a GTR + I + gamma
142 substitution model. The length of the simulated sequences and the evolutionary tree scaling rate
143 match each transmission pair's empirical sequence data. For this, we used previously estimated
144 empirically-derived within-host evolutionary rates (*42*) and the HXB2 sequence homologous to
145 the pair's sequence fragment as the ancestral sequence at the root. Every transmission pair
146 simulation produces a tip sequence alignment and a number of founder sequences equal to the
147 number of transmitted particles.
148
149 *Simulated topology class*: We reconstructed a phylogeny using maximum likelihood inference in
150 IQ-TREE 1.6.11 (*43*) and selected the best-fit nucleotide substitution model with ModelFinder
151 (*44*). Each phylogeny was classified as either MM, PM or PP (Supplementary Text).

Consequently, for each transmission pair k and each transmissibility model (i.e. number of viral particles founding infection of the recipient n_R), we generated a triplet of probabilities $M_{k,n_\mathrm{R}} = \{m_{k,n_\mathrm{R}}\}_{t\in T} = \Pr(t|k,n_R)\}_{\,t\in T}$ where $\sum_{t\in T}\Pr(t|k,n_\mathrm{R}) = 1$ and $T \in \{\mathrm{MM},\mathrm{PM},\mathrm{PP}\}$.

Transmissibility model calibration

For each transmission pair, we chose the most likely value of n_R (the number of virus particles founding each recipient infection) by matching the posterior topology class from the empirical phylogenetic transmission trees with the simulated distribution of topology class. Specifically, for each transmission pair, k, we estimated the most likely number of viral particles founding each recipient infection n_R^* as the n_R that maximises the multinomial likelihood function $L_{k,n_\mathrm{R}} = \Pr\left(D_k \,|M_{k,n_\mathrm{R}}\right) = \frac{N!}{\prod_{t\in T}(Nd_k(t))!}\prod_{t\in T} m_{k,n_\mathrm{R}}(t)^{Nd_k(t)}$. For each transmission pair k, we calculated lower and upper confidence limits for n_R^* as the minimum and maximum values of n_R that satisfy $L_{k,n_\mathrm{R}} > L_{k,n_\mathrm{R}^*} - 1.92$ and $L_{k,n_\mathrm{R}} < L_{k,n_\mathrm{R}^*} + 1.92$, respectively (*44, 45*). For each transmission pair k, we retain the best fit model for further analysis such that there are n_R^* viral particles founding infection of the recipient.

Haplotype analysis

Probability of a single founder haplotype: For each transmission pair, k, from the best fit transmissibility model, we defined the random variables F_S^k and F_R^k as the number of haplotypes that found infection of the source and the recipient partners, respectively. We then calculated the probability of there being a single founder haplotype in the recipient, stratified by topology class of the simulated phylogenetic tree (MM, PM, PP) and the number of founder haplotypes, *i*, in the

source partner, $p_i^k(t)$, that is, $p_i^k(t) = \Pr(F_R^k = 1 | F_S^k = i, t)$. Next, we defined the probability of a single founder haplotype in the recipient as a function of a tree topology, t, $p^k(t) = \Pr(F_R^k = 1 | t) = p_1^k \Pr(F_S = 1) + p_2^k \Pr(F_S > 1)$. By assuming that the source partners are randomly selected from the general MSM or HET population in which the probability of a single founder variant has been calculated to be approximately 0.7 (*14*), we set, $Pr(F_S = 1) = 0.7$ and $Pr(F_S > 1) = 0.3$. Finally, for each transmission pair, we calculated the probability of one founder haplotype given the observed triplet of empirical posterior topology classes D_k, as $q^k = \sum_{t \in T} p^k(t) d_k(t) / N$.

Number of founder haplotypes by source partner infection stage: We stratified all the transmission pairs into two sets by the infection stage of the source partner. We classified the acute transmission set as those pairs for whom recipient infection is within 90 days of source infection (a set of n_{acute} pairs), and the chronic transmission set as those pairs for whom recipient infection is 90 days or later after source infection (a set of n_{chronic} pairs). For each group, we calculated the mean probability of one founder haplotype being transmitted to the recipient in each set set as:

$$q^k_{\text{acute}} = \sqrt[n_{\text{acute}}]{\prod_{k \in \text{acute}} q^k}$$

$$q^k_{\text{chronic}} = \sqrt[n_{\text{chronic}}]{\prod_{k \in \text{chronic}} q^k}$$

Finally, we calculated the relative risk of one founder haplotype transmitted during the acute stage versus the chronic stage by $q^k_{acute} / q^k_{chronic}$.

Statistical analysis

We compare our results by using statistical tests and report the respective *P*-values. To compare

Supplementary Text

Transmission pairs sequence data

Our alignments are provided at github.com/AtkinsGroup**.**

On average, 22 (IQR 13-33) HIV sequences are obtained from the source and 21 (IQR 10-20) sequences from the recipient for the MSM pairs, and 21 (IQR 12-25) and 18 (IQR 9-22) for the HET source and recipient, respectively. All MSM sequence data belong to subtype B, while most heterosexual sequence data belong to subtype C (49%), followed by subtype B (22%), subtype D (21%), subtype A/A-like (7%) and unclassified subtype (1%). A total of 7 (19%) of the MSM pairs have near full genomes sequenced and the remaining pairs had *env* available (mean 1653 nt, range 182-3827 nt). Ten (13%) of the HET pairs had near full genomes available, while 56 (75%) pairs had *env* (mean 1321 nt, range 323-2582 nt), nine (12%) pairs had either *pol* or *gag* (mean 1484 nt, range 1375-1499 nt) and one pair had vif-LTR3 (4666 nt) sequenced.

212

213 **Effect of number of founding virus particles in the source**

214 To assess whether the number of founding virus particles in the source partner affects the
215 diversity of sequences founding infection in the recipient, we model a scenario where the index
216 case transmitted one, two or six virus particles to the source partner at either one or three year(s)
217 after infection. The source in turn transmits 1 to 6 virus particles to the recipient at 30 days
218 (acute) or 1095 days (chronic) later. The simulation produces a dated viral phylogeny with tips
219 sampled at either 30 (early) or 1065 days (late). We model 1kb nucleotide sequences along the
220 simulated viral phylogenies using the same method as in the main text.
221
222 The genetic variation rapidly and steadily increases over time – the maximum diversity among
223 transmitted haplotypes to the recipient was higher when the index case was infected for longer
224 and the transmission to the recipient occurs during the chronic stage of the source (**Fig. S2**).
225 When the source has more than one founding particle, this leads to a bimodal distribution of
226 maximum diversity among transmitted founder variants within the recipient. The first and second
227 mode represent maximum diversity when drawing the recipient founder haplotypes from either
228 one or more than one viral population within the source, respectively. However, increasing the
229 number of founding virus particles to more than two within the source only increases the density
230 around the second mode without affecting the range of the maximum diversity distribution. This
231 consistency occurs because increasing the number of founding virus particles in both
232 transmission partners, increased the probability of drawing founding variants from different
233 genetic pools in the source. However, the average maximum diversity of the founder variants

does not change because the source genetic pools evolved at the same rate and under the same evolutionary constraints with no selective advantage. This leads to genetic pools with equivalent cumulative genetic change but distinct identity. Taking this into account, we chose to model one or two founding virus particles within the source partner as we were interested in capturing some degree of variation in the transmitted haplotypes rather than multiple genetic identities *per se*.

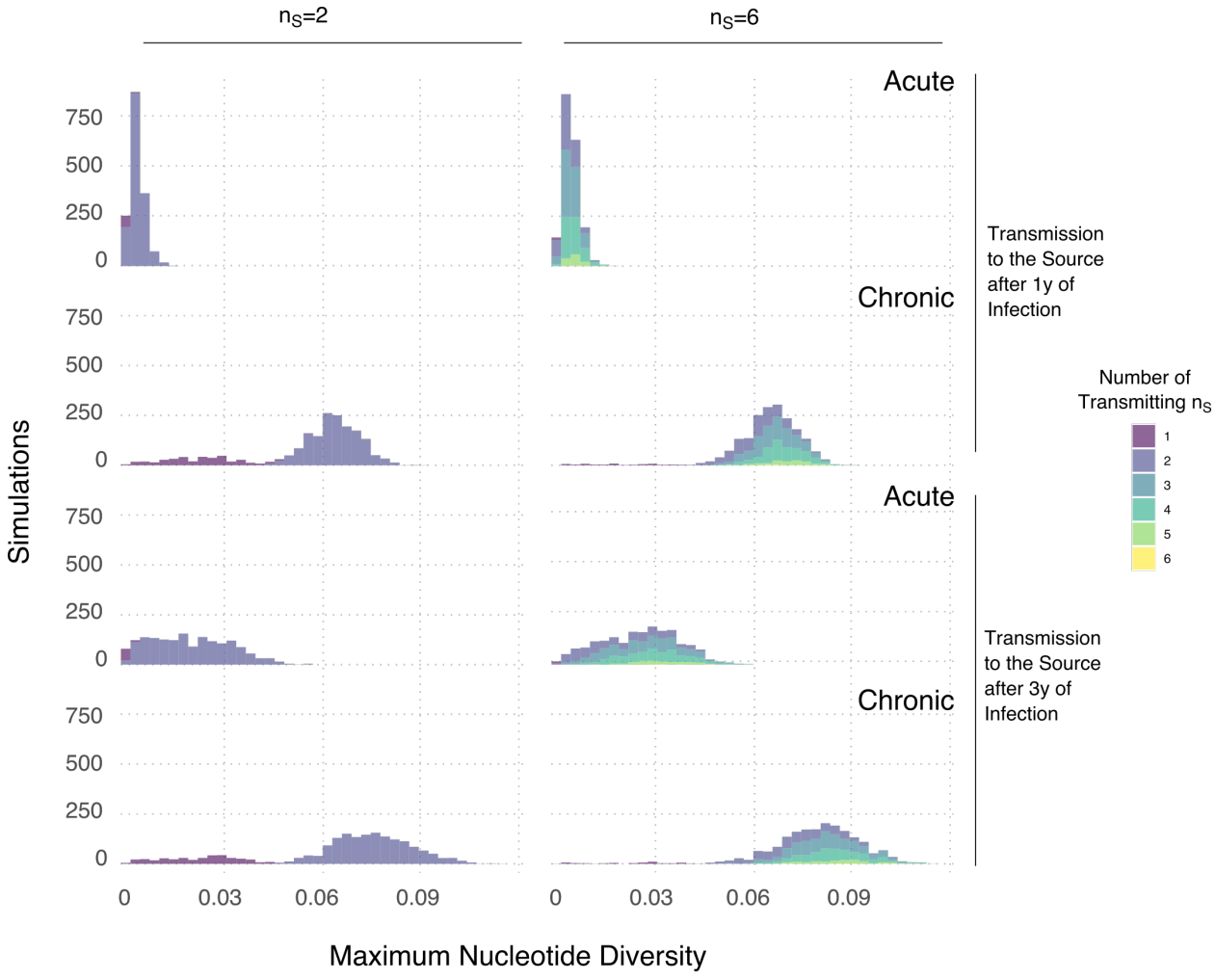

Fig. S2: Effect of number of founding virus particles in the source.

Effect of using a confidence threshold for assigning the topology class

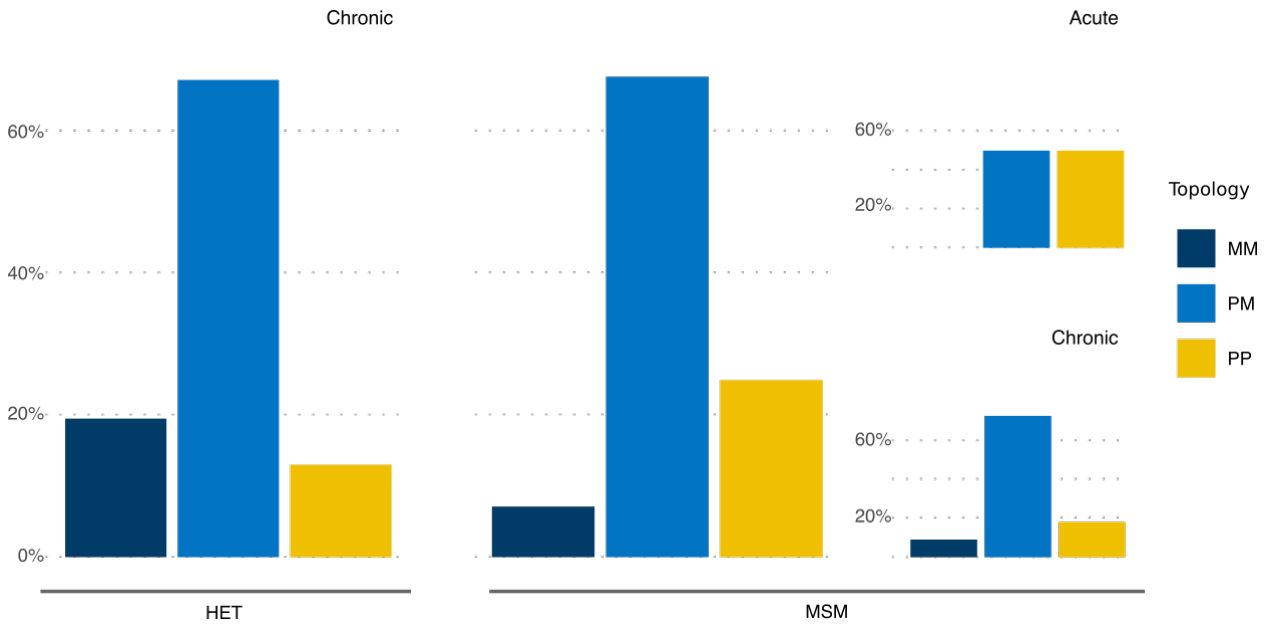

Fig. S3: Phylogenetic findings of the empirical transmission pairs for whom the posterior trees gave a certainty of over 95% for the most frequent topology. Fraction of phylogenetic tree topology class (MM - Monophyletic-Monophyletic, PM - Paraphyletic-Monophyletic and PP - Paraphyletic-Polyphyletic) where each tree topology class is classified as the most frequent topology class of each posterior distribution per transmission pair. Results are stratified by risk group: 76 heterosexual (HET) pairs and 36 men-who-have-sex-with-men (MSM) pairs) and infection stage of the source partner at transmission (11 acute pairs defined as <90d post infection and 101 chronic pairs defined as ≥90d post infection).

Effect of index partner stage of infection at transmission

In the main analysis we assumed that all index cases transmit to the source partner after three years of infection. Here we also evaluated the results assuming the transmission risk was skewed towards early infection, with half of all simulations across all transmission pairs assuming index case transmission occurs during the acute stage (≤90d) and half occurs during the chronic stage (91d-3y). We find qualitatively similar results as our main analysis. The median number of founder variants transmitted across all pairs is 1 (range: 1-5, **Fig. S4A**). Across all pairs in both risk groups, the mean probability of observing one founder variant is 0.73. Stratifying by risk group, we find there is a higher probability that one variant founds HET infections than MSM infections (a geometric mean of 0.79 vs. 0.61, **Fig. S4B**). In contrast, when stratifying solely by infection stage of the source partner, we find that transmission during the acute stage has a much lower probability of one founder variant than during the chronic stage (means of 0.38 vs. 0.78) with a higher median number of founder variants transmitted, when only the most likely number of transmitted founder variants for each pair is considered (2 vs. 1, **Fig. S4A**). From these results, therefore, there is still approximately twice the chance of multiple founder variant transmission during acute stage infection across both risk groups (relative risk is 0.48).

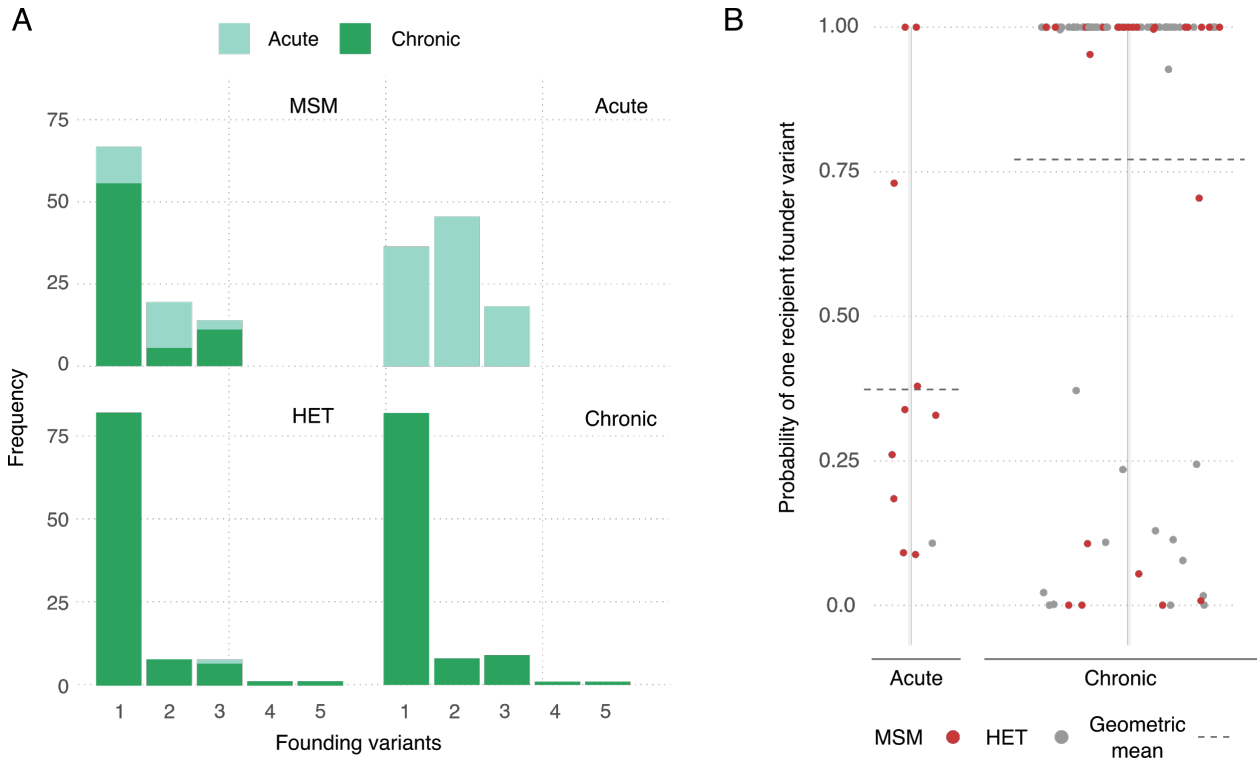

Fig. S4: Phylogenetic findings from the calibrated simulations with skewed transmission rate towards acute stage for the index case. A) Frequency of the number of founder variants for transmission pairs by infection stage of source partner at transmission and risk group. The number of transmitted founding variants is calculated as the modal simulated value. B) Probability of one founder variant in the recipient for each pair stratified by infection stage of the source partner at transmission.

Effect of constructing empirical data phylogenetic trees using maximum likelihood inference with bootstrapping

In the main analysis we used Bayesian phylogenetic reconstruction to analyse the empirical sampled genetic data of each empirical transmission pair**,** using the respective posterior distribution to calculate the frequency of each topology class (MM, PM and PP). Here we

provide a sensitivity analysis to calculate the tree topology class distribution of the empirical sampled genetic data by maximum likelihood phylogenetic tree construction and bootstrapping. After bootstrapping the empirical data 100 times to calculate the frequency of MM, PM and PP topology classes for each transmission pair, we then proceeded using the same methodology as in the main text. That is, we fit the simulation model (parameterised with the pair-specific data) to the bootstrapped data individually for each transmission pair by comparing the frequencies of tree topology classes. Overall our results remained consistent with our main results, albeit with slightly lower probabilities of observing one founder variant. The median number of founder variants transmitted across all pairs is 1 (range: 1-11, **Fig. S5A**). Across all pairs in both risk groups, the mean probability of observing one founder variant is 0.62. Stratifying by risk group, we find there is a higher probability that one variant founds HET infections than MSM infections (a geometric mean of 0.67 vs. 0.53, **Fig. S5B**). Stratifying by infection stage of the source partner, we find there is a much lower probability of one founder variant during the acute stage than during the chronic stage (means of 0.31 vs. 0.66) with approximately twice the chance of multiple founder variant transmission during acute stage infection across both risk groups (relative risk is 0.47).

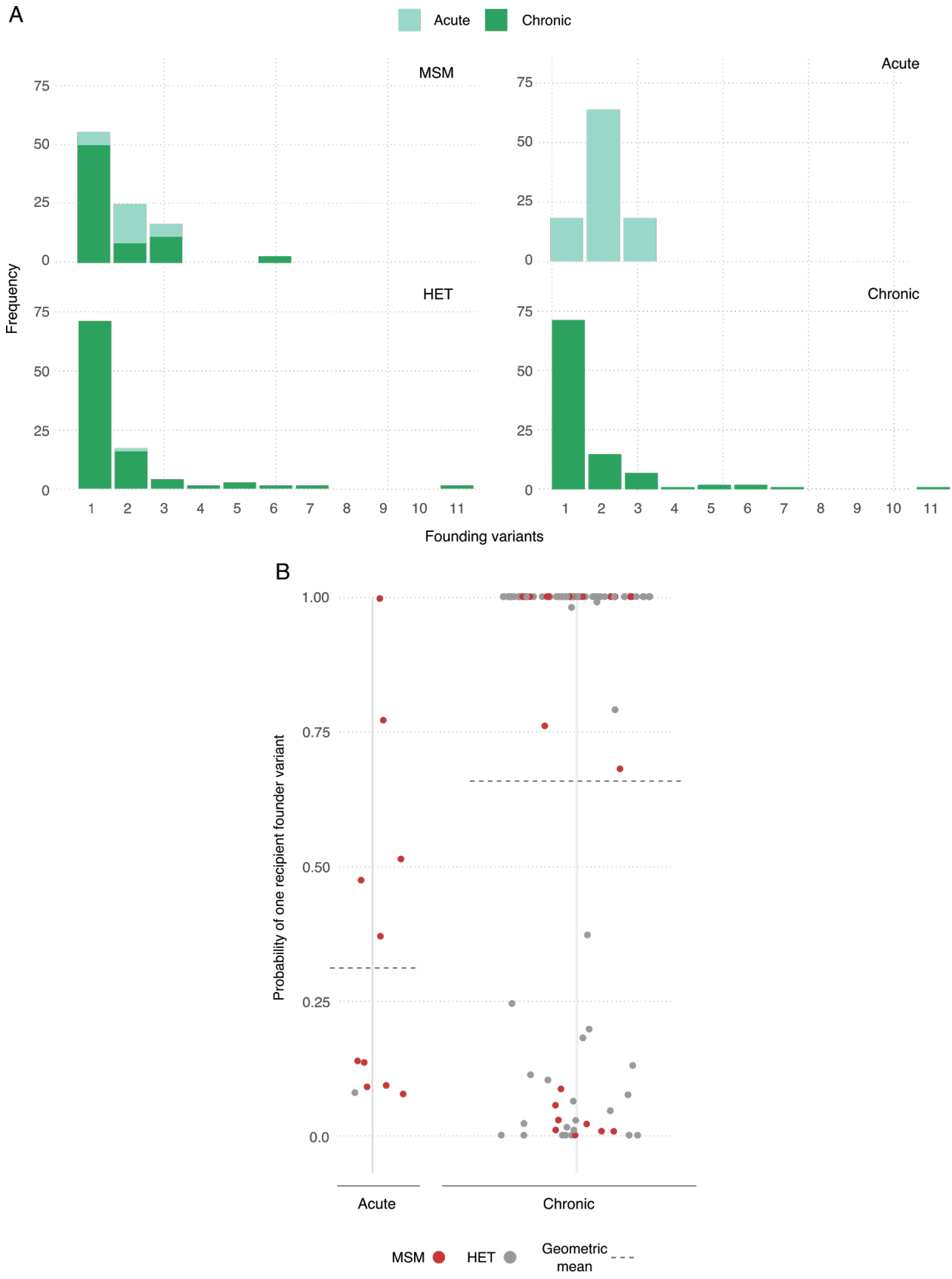
A
Acute
Chronic
MSM
Acute
HET
Chronic
Frequency
75
50
25
0
1
2
3
4
5
6
7
8
9
10
11
Founding variants
B
Probability of one recipient founder variant
1.00
0.75
0.50
0.25
0.0
Acute
Chronic
MSM
HET
Geometric mean

302

Fig. S5: Phylogenetic findings from the calibrated simulations with bootstrapped empirical data. A) Frequency of the number of founding variants for transmission pairs by infection stage of source partner at transmission and risk group. The number of transmitted founding variants is calculated as the modal simulated value. B) Probability of one founder variant in the recipient for each pair stratified by infection stage of the source partner at transmission.

Effect of the number of sequences for each transmission pair

Here we provide sensitivity analysis to the estimation of the probability that a single founder variant was transmitted to the respective recipient by the number of sequences available from the source and recipient, which ranges from 5 to 149 across all partners. First, the number of sequences available from the transmitter and the recipient is correlated (*Pearson's* product-moment correlation=0.53, $P<0.01$). However, we do not find any evidence of correlation between the total number of sequences for a pair and the estimated number of founder variants in the recipient ($P>0.2$). While an MM topology is more frequently observed when the total number of sequences was small ($P<0.01$), removing the pairs with a likely MM topology do not change our main result: the probability that a single founder variant was transmitted to the respective recipient is lower for the acute pairs (0.402) than for the chronic ones (0.749).

Effect of the sequencing method

We evaluated if our results were affected by the type of sequence data used in the analysis. All of the transmission pair data were generated using Sanger capillary sequencing except for those in one study ((*46*) in **Data S1)** which used Illumina sequencing on end-point diluted primary isolates. Our results are robust to the exclusion of the eight transmission pairs extracted from this

study: that is, the probability that a single founder variant is transmitted to the respective recipient is lower for the acute stage (0.402) than for the chronic stage (0.756).

Effect of the gene region and length

Looking at chronic stage transmissions only, if we compare the number of founder variants inferred from envelope gene sequences to those inferred from non-envelope sequences, we don't find significant differences ($P>0.4$) in the probability that a single founder variant is transmitted to the respective recipient: 0.739 for envelope sequences and 0.856 for non-envelope ones. Conversely, if we include data from both chronic and acute transmissions, and restrict our analysis to those pairs with sequences from the envelope region, our results remain unchanged. That is, the probability that a single founder variant is transmitted to the respective recipient is lower during the acute stage (0.432) than during the chronic stage (0.739). Finally, if we condition our analysis on those pairs for whom full or near full genomes are available (17 pairs), our results remain consistent with the main analysis: the probability that a single founder variant was transmitted is lower for acute stage transmissions (0.138, n=1) than for chronic stage transmissions (0.903, n=16). We found that length of the sequenced region is not correlated with the probability that a single founder variant is transmitted to the recipient (*Pearson's* product-moment correlation=0.14, $P>0.14$). Moreover, there are no significant differences ($P>0.81$) in the length of the sequenced region when stratifying our data by infection stage of the source partner at transmission. Together these observations indicate that our results are not influenced by the length of sequenced regions.

Data S1 (Separate file): SITable_EpiGeneticData.csv. Collated epidemiological and clinical data and genetic metadata for the 112 transmission pairs used in the analysis.

Data S2 (Separate file): SITable_AnalysisData.csv. Analysis information for the 112 transmission pairs used in the analysis.

Data S3 (Separate file): SITable_ColumnNamesKey.csv. Additional information on column headers in Data S1,S2 tables

Data S4 (Separate file): Alignments.zip. Individual files of sequence alignments used in the analysis for the 112 transmission pairs.